Behavior Research Methods (2023) 55:38–57
https://doi.org/10.3758/s13428-021-01783-3

A simple method for comparing peripheral and central color vision by means of two smartphones

Galina Rozhkova[1] · Alexander Belokopytov[1] · Maria Gracheva[1] · Egor Ershov[1] · Petr Nikolaev[1]

Accepted: 24 December 2021 / Published online: 8 March 2022

Abstract

Information on peripheral color perception is far from sufficient, since it has predominantly been obtained using small stimuli, limited ranges of eccentricities, and sophisticated experimental conditions. Our goal was to consider the possibility of facilitating technical realization of the classical method of asymmetric color matching (ACM) developed by Moreland and Cruz (1959) for assessing appearance of color stimuli in the peripheral visual field (VF). We adopted the ACM method by employing two smartphones to implement matching procedure at various eccentricities. Although smartphones were successfully employed in vision studies, we are aware that some photometric parameters of smartphone displays are not sufficiently precise to ensure accurate color matching in foveal vision; moreover, certain technical characteristics of commercially available devices are variable. In the present study we provided evidence that, despite these shortages, smartphones can be applied for general and wide investigations of the peripheral vision. In our experiments, the smartphones were mounted on a mechanical perimeter to simultaneously present colored stimuli foveally and peripherally. Trying to reduce essential discomfort and fatigue experienced by most observers in peripheral vision studies, we did not apply bite bars, pupil dilatation, and Maxwellian view. The ACM measurements were performed without prior training of observers and in a wide range of eccentricities, varying between 0 and 95°. The results were presented in the HSV (hue, saturation, value) color space coordinates as a function of eccentricity and stimulus luminance. We demonstrated that our easy-to-conduct method provided a convenient means to investigate color appearance in the peripheral vision and to assess inter-individual differences.

Keywords Peripheral vision · Color vision · Asymmetric color matching · Smartphones in visual research

Introduction

In natural viewing conditions, the human visual system integrates input signals from the central and peripheral retina, creating a single perceived image of the whole visual field (VF).

It is well known that the sensory surface that receives the optical inputs from all parts of the VF—the retina—has a very heterogeneous structure. This implies that when visual stimuli fall onto different spatial locations in the retina, the same visual task has to be solved by recruiting different neuronal "units" and mechanisms. Such a situation has stimulated comparative studies of the visual processes at the center and periphery of the VF, in particular concerning color perception.

However, it does not mean that the characteristics of central and peripheral color vision have been studied equally well, since investigation of the peripheral vision is much more difficult (Abramov & Gordon, 1977; Moreland, 1972; Neitz & Jacobs, 1990; Rozhkova, Belokopytov, & Iomdina, 2019a). In everyday life, one's attention is usually directed to the central area of the VF, leading to preferential processing of the central visual stimuli, while the experiments aimed at investigation of the peripheral vision require changing the habitual viewing mode and drawing attention to the peripheral stimuli. This explains why the majority of reliable studies of peripheral vision were performed after special training of participants.

To date, the number of reliable studies of peripheral color vision is rather small and is insufficient for us to draw a complete picture of it. This indicates the need for new findings and also motivates the development of novel experimental

✉ Galina Rozhkova
gir@iitp.ru

[1] Institute for Information Transmission Problems, RAS, Bolshoy Karetny 19, 127051 Moscow, Russia

procedures. Such demand is increasing in view of the recent discovery of new light-sensitive elements in the human retina, *melanopsin*-expressing intrinsically photosensitive retinal ganglion cells (ipRGCs), which are considered to contribute to color perception as well (Graham, 2014; Graham et al., 2007; Zele et al., 2018).

One of the traditional methods for assessing peripheral color vision is asymmetric color matching (ACM), proposed more than 60 years ago (Moreland & Cruz, 1959) and widely used in many investigations up to now (Stabell & Stabell, 1976, 1979, 1982a, 1984, 1996; McKeefry et al., 2007; Murray et al., 2012; Opper et al., 2014; etc.). A classical color matching paradigm (e.g., realized in the Wright colorimeter) implies perceptual equalization of the two colors presented on the two halves of the colorimeter screen by properly adjusting the reference light composed of the three monochromatic light beams, the colorimeter primaries. In the Moreland and Cruz ACM procedure, a visual match is accomplished between one stimulus imaged on the central part of the retina and another stimulus projected onto the peripheral part of the retina.

The two matching procedures are based on the assumption that human color vision is trichromatic. This is shown to be true at least of the foveal color vision under daylight (photopic) conditions when color perception is determined by inputs of the three types of cone photoreceptors. However, in a general case, one needs to take into account other photosensitive retinal elements involved in color vision. By now it is established that, at different light conditions and for different regions of the VF, various retinal cells selectively sensitive to different wavelengths contribute to human color perception: three types of cones determining daytime color vision and contributing to twilight vision (short-wave S-cones, with peak sensitivity at ~430 nm; middle-wave M-cones with peak sensitivity at ~530 nm; and long-wave L-cones with peak sensitivity at ~560 nm); rods, the receptors much more sensitive to light than cones (with peak sensitivity between S- and M-cones at ~520 nm) enabling night vision and contributing to twilight vision; and ipRGCs containing melanopsin with peak sensitivity between rods and S-cones (at ~ 490 nm). The number of publications on ipRGCs and their possible contribution to visual functions is rapidly growing (Berson et al., 2002; Hattar et al., 2002; Dacey et al., 2005; Graham, 2014; Cao & Barrionuevo, 2015; Baraas & Zele, 2016; Hannibal et al., 2017; Zele et al., 2018; Schroeder et al., 2018; Allen et al., 2019; Spitschan, 2019; Yamakawa et al., 2019, etc.).

Figure 1A presents information on the spectral sensitivity of these retinal elements (gray curves); superimposed are the monochromatic primaries used in the classical Wright colorimeter (colored bars).

It is well known that distribution of the light-sensitive cells over the human retina is very inhomogeneous (Curcio et al., 1987, 1990; *Østerberg*, 1935), as illustrated by Fig. 2. Cone density is greatest at the retinal center (fovea) and decreases with eccentricity very steeply up to 3° (point 1 on the corresponding curve in Fig. 2); in the range of 3°–10° (between points 1 and 2 in Fig. 2), the decrease is less; at the interval 10°–80° (between points 2 and 3), the decrease is very slow, and at the retinal edge (point 4), near the ora serrata, there is a significant increase in cone density, known as the cone-enriched rim (Mollon et al., 1998; To et al., 2011; Williams, 1991). In comparison, rod density has its peak at the mid-periphery of the retina. Moreover, rod density as a function of eccentricity varies substantially for different radial directions. For instance, in the nasal part of the horizontal meridian, the peak rod density is confined to the range of 10°–20° (over the $120 \times 10^3/\text{mm}^2$, indicated in Fig. 2) compared to the range of 15°–40° in the temporal part of this meridian.

Currently the data on the distribution of the ipRGCs in the human retina are very preliminary. One can only be sure that the ipRGCs are absent in the central 2° of the retina since, in this area, all ganglion cells are moved aside to the edges of the foveola (Polyak, 1941; Schein, 1988).

Many ophthalmologists and some visual scientists still share the last century's notion that, with increasing eccentricity, there is a transition from normal trichromatic vision to dichromatic vision, and finally to achromatic vision (color blindness) at the far periphery. Sixty years ago, such an opinion was clearly formulated by Moreland and Cruz, whose paper (1959) had influenced peripheral vision studies for many years. The authors estimated the appearance of the peripheral test color by matching it to a foveal mixture field (i.e., by asymmetric color matching method [ACM] proposed in this research) and concluded that "the results indicate a progressive deterioration in colour perception with distance from the fovea: tending, under the conditions of the experiment, to dichromatism at 25°–30° and to monochromatism at 40°–50°" (Moreland & Cruz, 1959, p. 117). The data that justified their conjecture were obtained for two observers (the authors) under dark adaptation, monocular (right eye) viewing, and the observer's head stabilized by a dental plate mounting. The test and comparison stimuli (80 min × 40 min) were presented simultaneously as pulses of 0.5 s duration, every 2 s. The position of the test stimulus was varied from 10° to 30° in the lower vertical meridian and from 15° to 50° in the nasal horizontal meridian. Although the authors explicitly indicated that their conclusions were based on the data obtained "under the conditions of the experiment," their view of the degraded peripheral color vision was often improperly generalized by successors in this field of research.

However, numerous post-1959 studies demonstrated that the elaborated conceptions of peripheral color vision required profound revision. On one hand, many authors

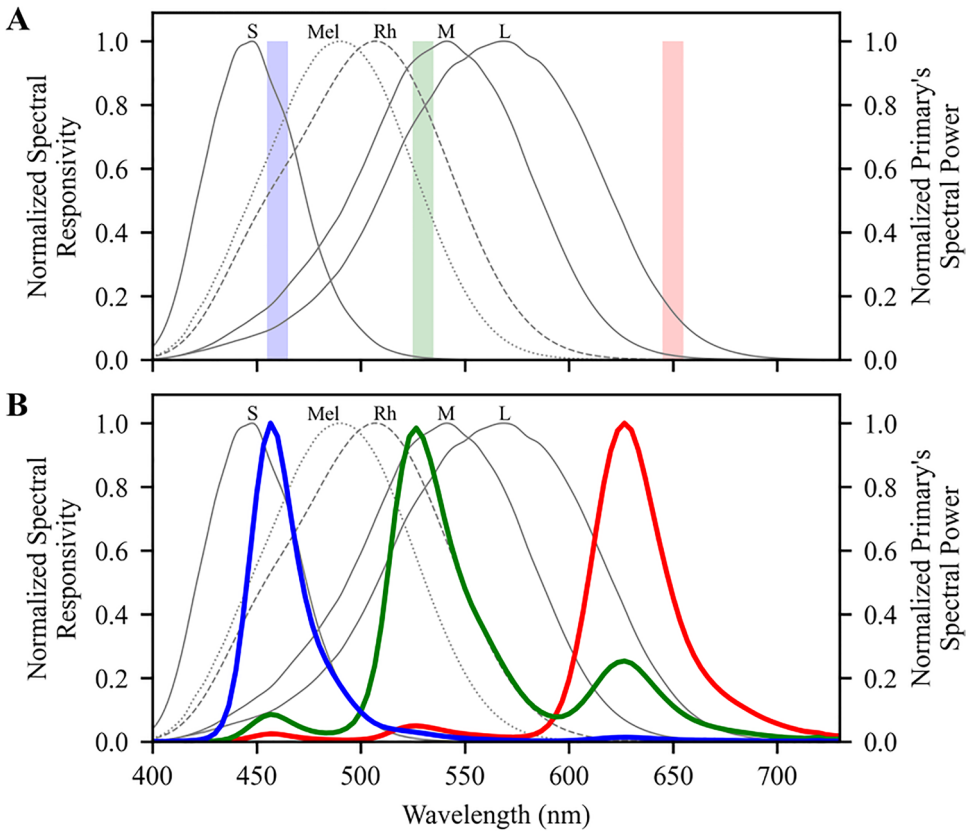

Fig. 1 **A** The spectral sensitivity curves of rods (Rh), cones (S, M, L), and melanopsin ganglion cells (Mel) in the human retina according to data from the Commission Internationale de l'Eclairage [CIE], 2018. The three colored bars indicate the Wright primaries (Wright, 1929) commonly used in colorimetric experiments—monochromatic beams of 650, 530, and 460 nm (each of 10 nm width). **B** Spectral characteristics of the smartphone (Samsung Galaxy S8) RGB primaries (colored curves) used in the present experiments as proxies of the Wright primaries and superimposed on the spectral characteristics of the color-sensitive elements in the human retina

continued to develop the main existing conceptions and performed studies using relatively small equal stimuli for the foveal and the peripheral locations to investigate the suggested color vision deficiency at the periphery of the human VF in greater detail and to describe degradation of color perception mechanisms with increasing stimulus eccentricity. The earlier advancements of such studies were summarized in a voluminous review by J. Moreland (1972). Later, the conceptions of color vision degradation with increasing stimulus eccentricity were further developed and refined in many studies on the basis of assessing color appearance, measuring color detection and discrimination thresholds, comparing the activity of L-M and S-(L+M) channels, investigating the effects of light adaptation and stimulus velocity (Rozhkova & Yarbus, 1974; Yarbus & Rozhkova, 1977; Stabell & Stabell, 1976, 1979, 1982a, 1982b, 1984, 1996, 2002; Abramov & Gordon, 1977; Gordon & Abramov, 1977; Greenstein & Hood, 1981; Noorlander et al., 1983; Ambler, 1974; Abramov et al., 1991; Nagy & Wolf, 1993; Parry et al., 2006, 2012; McKeefry et al., 2007; Hansen et al., 2009; Panorgias et al., 2012; etc.). These studies clarified many details and important features of the peripheral color vision mechanisms as well as the causes of their apparent deficiency in comparison to the foveal mechanisms.

On the other hand, these studies demonstrated essential (in certain cases, even crucial) dependence of the results on the stimulus parameters (size, intensity, velocity, exposure duration, etc.) and experimental conditions (level of ambient illumination; type, duration, specific phase of adaptation; methods of measurement; etc.). With time, authors increasingly mentioned that in certain conditions, the color vision in the periphery could be nearly as good as that in the foveal area. To illustrate this tendency, it is worth mentioning several investigations employing various methods.

Studying the effects of stimulus movement on the peripheral vision (detection, resolution, and color discrimination thresholds) in natural photopic viewing conditions, Rozhkova and Yarbus (1974) revealed that the stimulus velocities optimal for a clear vision were dependent on eccentricity. The stimuli were Landolt C and colored circles (drawn on white paper) of varying size (from 1/3° to 3°) moving with varying velocity (0°–100°/s) at eccentricities of 0°–70°. At

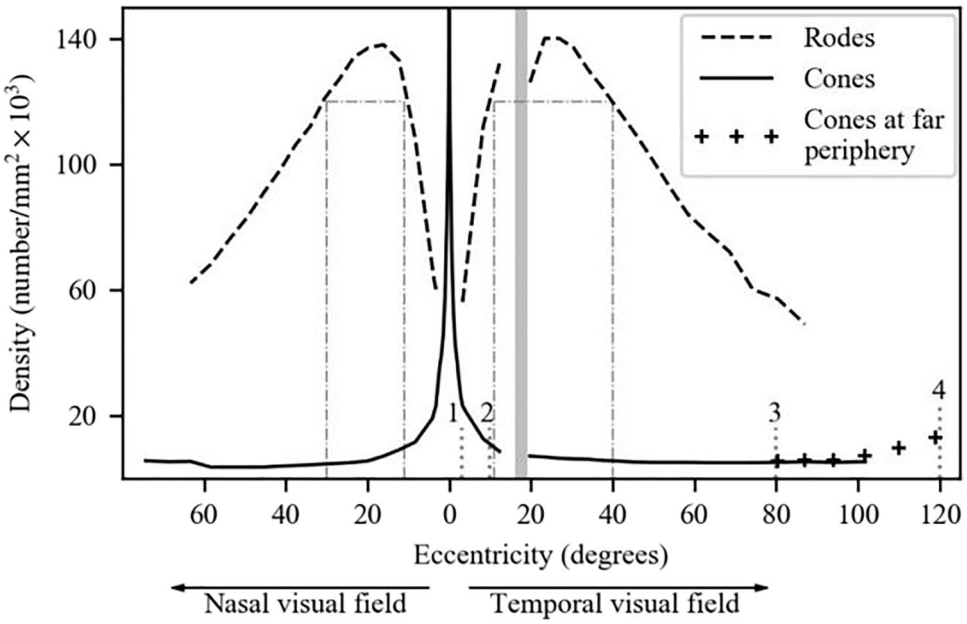

Fig. 2 Inhomogeneous distribution of rods and cones in the human retina. Schematic illustration (based on *Østerberg*, 1935; Curcio et al., 1990). The points 1, 2, 3, and 4 correspond to the ends of the intervals with different cone density gradients. Dash-dotted vertical lines indicate widths of rod peak zones in the nasal VF (temporal retina) and the temporal VF (nasal retina) along the horizontal meridian; gray bar indicates position of the blind spot

any position in the studied part of the VF, it was possible to determine the stimulus size and velocity providing near normal perception of the stimulus shape and color.

In the paper by Noorlander et al. (1983), presenting detection thresholds for spatiotemporal color contrast modulation, the authors wrote: "For constant target size, colour vision deteriorates if the stimulus is moved away from the fovea, but if the shift is combined with a suitable enlargement of the target size, colour discrimination at the periphery is comparable to that at the fovea" (p. 1). In this investigation, the stimulus sizes ranged from 1/8° to 16°, and the eccentricities used were 0-2-6-15-21-50°.

McKeefry and coauthors (2007), describing their data on the decrease in the L-M channel signal with eccentricity (based on presenting the same stimuli of 3° at eccentricities of 12°, 18°, and 24° and also stimuli varying in size from 2° to 5° at eccentricity of 18°), noted that "…changes in perceived saturation readily apparent for the smallest stimulus sizes, are greatly reduced with increasing stimulus size" (p. 3173).

In the paper by Volbrecht and Nerger (2012), presenting hue-scaling data for circular (0.25°–5°) monochromatic stimuli at eccentricities of ±10° along the vertical and horizontal retinal meridians in bleach and no-bleach conditions (to change rod contribution), the authors noted: "As stimulus size increases…, the differences in hue perception among the four peripheral locations and the two bleach conditions are attenuated" (p. A44).

Regarding the importance of the stimulus size, the most general statement was formulated by van Esch and his coauthors: "If field-size scaling according to the eccentricity-dependent cone density, the cortical magnification factor, or the reciprocal of the interganglion cell distance is applied, then wavelength-discrimination performance from 8 degrees to 80 degrees eccentricity is roughly the same." (van Esch et al., 1984, p. 443). Similar statements could also be formulated for other stimulus parameters and viewing conditions. Thus, it seems reasonable to think that, at present, the nearest aim in studying the peripheral vision is to find the conditions for nearly normal viewing at each eccentricity and to describe limitations and characteristics of the inferior "distorted/defective" images observed in other conditions.

To date, the majority of studies on peripheral color vision report data obtained at rather unnatural and highly specific conditions (Maxwellian view; specific adaptation procedures; limited ranges of eccentricities, stimulus size, luminance, temporal parameters, ambient illumination levels, etc.). It is therefore hardly surprising that under different experimental conditions, quite different phenomena were recorded and, thus, different (even opposite) conclusions were drawn.

For instance, one might compare the following conclusions drawn by several authors about perceived saturation of the peripheral stimuli:

(1) "The quality of color vision in the periphery depends crucially on stimulus size. If the stimulus is sufficiently large, subjects see a full range of well saturated hues." (Gordon & Abramov, 1977, pp. 205–206);
(2) "In agreement with previous studies the results show that the saturation of the different colours is reduced when the monochromatic stimuli are moved from the fovea toward the periphery" (Stabell & Stabell, 1976, p. 1100);
(3) "Foveal and peripheral hue-scaling data were obtained for a 1° foveal stimulus and a 3° stimulus presented at 10° retinal eccentricity under both bleach (reducing rod input) and no-bleach (permitting rod input) conditions. … Peripheral stimuli appeared more saturated than foveal stimuli (i.e., supersaturated), especially in the green–yellow region. This effect was particularly pronounced for the peripheral bleach condition" (Opper et al., 2014, p. A148).
(4) "The task for the observers was to match a peripheral 3°- spot at 18°- eccentricity in the nasal VF with a parafoveal 1°- probe spot (1°- eccentricity, nasal VF) in hue and saturation. For both males and females, there is greater saturation loss in the green region with males exhibiting higher loss. Females show a slightly greater saturation loss in the red region of the color space" (Murray et al., 2012, p. 3).

The above quotations make the available data seem like a collection of disjointed fragments of information in a puzzle with too many tiles absent, which precludes working out a complete view of the peripheral color vision.

From the viewpoint of ecological validity, the main hindrance in understanding the peripheral color vision phenomena is a lack of data obtained under natural viewing conditions and by accessible methods. The traditional lab-based investigations of the peripheral color vision have their limitations, such as the technically elaborate Maxwellian view, expensive equipment required for colorimetric measurements, and long-lasting and complex adaptation procedures, i.e., factors that limit research potential to acquire richer information on the topic.

The development of an experimental technique that is accessible and affordable for wide application seems to be feasible, since it opens new avenues to enhance investigation of the peripheral vision. Building upon the requirements of accessibility and broad applicability, we developed an easy-to-handle setup with two off-the-shelf smartphones for conducting a pilot study to compare and match the appearance of colors presented centrally and in the periphery of the VF. Although we are aware that off-the-shelf smartphones are not quite suitable for performing precise measurements, we reckon that they are convenient for a rapid assessment of certain characteristics of matched colors and for demonstration of certain phenomena of peripheral color vision.

In our experiments, we employed smartphones to implement the ACM procedure. Figure 1B shows the spectral characteristics of the smartphone primaries which are proxies of the three monochromatic beams (Fig. 1A) used as the primaries in the classical Wright colorimeter. As one can see, the bandwidths of the smartphone primaries are much wider and the spectrum of the green primary has significant side peaks. However, from a theoretical viewpoint, such particularities are not crucial in colorimetry (the first law of Grassmann only requires linear independence of the primaries [MacAdam, 1970; Wyszecki & Stiles, 1982]).

This paper consists of the main part, presenting methods and results, and the supplement containing more specific technical data. The Methods section provides information on technical and photometric characteristics of the employed smartphone that are essential for the present study, details of the experimental setup, and the ACM procedure. The Results section presents our findings on the appearance of color stimuli at the periphery of the VF as matched to those observed in the fovea. This section contains both novel data and results that confirm some earlier outcomes in studies employing more sophisticated lab equipment and procedures, and trained observers.

Some of our experiments and measurements were carried out to clarify certain technical issues concerning the effects of the smartphone temperature, temporal properties of the stimuli, benign differences in spectral characteristics of the test and reference devices, etc. Outcomes of these auxiliary experiments are presented in the Supplement.

Methods

The experimental setup

Our main experiments were carried out using a pair of smartphones with supposedly identical characteristics and a modified commercial mechanical perimeter PNR2 (analogous to the Förster perimeter) with an arc radius of 33 cm. The basic setup is shown in Fig. 3A. The smartphone for the peripheral test stimulus presentation was attached to a platform that could be moved over the elongated perimetric arc to vary the eccentricity of test stimuli. The second smartphone was fixed at the center of the perimetric arc (at zero eccentricity) for displaying the reference color stimulus.

The peripheral smartphone was connected to a notebook for test stimulus generation and setting its parameters. Stimulus parameters on the central smartphone could be varied by manipulation with a mouse connected to this smartphone. Quantitative characteristics of the displayed color were expressed in the HSV (hue, saturation, value) color

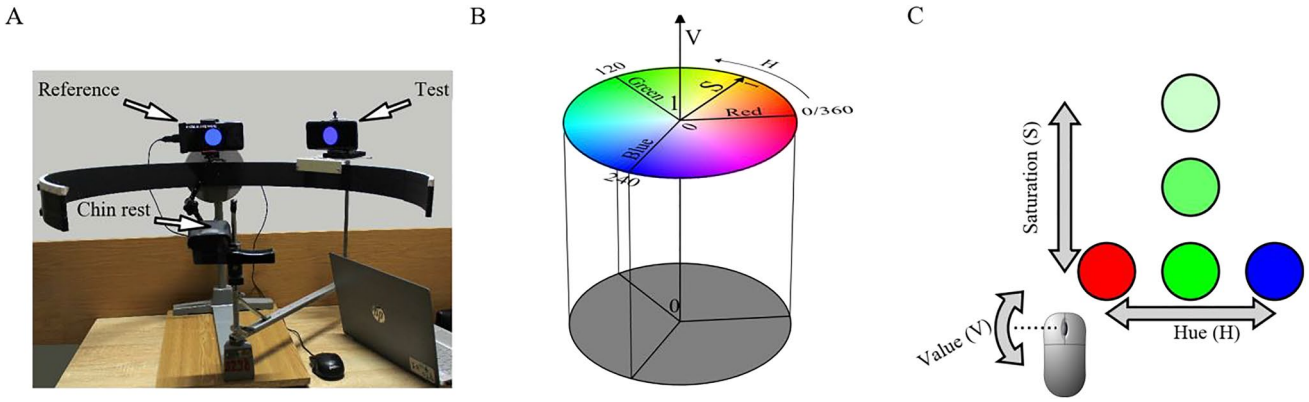

Fig. 3 **A** Experimental setup for color matching: photo of the perimeter with two smartphones for displaying test and reference stimuli. **B** Schematic representation of the HSV color coordinate system used in this investigation. **C** Scheme of adjusting reference stimulus color by manipulations with mouse

coordinate system. (Some reasons in favor of using the HSV color space in our experiments are given below; a schematic representation of the HSV color space is shown in Fig. 3B.) The observers had to match the central reference stimulus to the peripheral test stimulus in hue (H), saturation (S), and brightness (V). This matching was achieved by moving the mouse in different directions (to vary H and S) and rotating the mouse scroll wheel (to vary V) (Fig. 3C).

The software for color stimulus generation on the smartphones was developed using JavaScript (the source code is accessible on https://github.com/abelokopytov/spot).

The choice of the color coordinate system

For estimation of color appearance, we preferred using the well-known HSV color coordinate system elaborated in the 1970s (Joblove & Greenberg, 1978; Smith, 1978; Wyszecki & Stiles, 1982), although since that time many other color coordinate systems have been developed for various visual tasks and applications.

For our investigation, the type of color coordinate system was not crucial. To make the color choice easier and faster and, hence, to reduce the duration of the matching experiments, the following requirements seemed to be reasonable:

(1) The system should be designed for image visualization on displays and should meet the characteristics of smartphones providing representation of all possible colors (smartphone color gamut).
(2) The system should be easy to understand by naïve observers; i.e., it should be correlated with visual perceptual qualities of color encountered in common use—hue, saturation, and brightness/lightness.
(3) It is desirable to separate the control of image chromaticity from image intensity and to provide simple adjustment of color stimulus by mouse (e.g., movements of the mouse over the table may determine changes in chromaticity, and turning the mouse wheel, changes in brightness).
(4) The system should be suitable for the meaningful association of different mouse movements with the adjustment of different chromaticity parameters (e.g., left–right directions of movement with hue changes, and forward–backward directions with saturation changes).

The HSV color coordinate system belongs to the RGB (red, green, blue) class. In general, color systems of the RGB class are more suitable than others for the images generated on displays. This class includes about a dozen versions. However, most of them do not fit one or more of our requirements. In particular, the CMY (cyan, magenta, yellow) and CMYK (cyan, magenta, yellow, key) systems do not meet point (1) because they are developed for printed images. Requirement (3) excludes the widely used systems RGB, YUV, and ICtCp since, in these systems, each of the three free parameters influence stimulus chromaticity. By taking into account requirement (4), the list of candidates is shortened to HSV and several rarely used color coordinate systems. In such a situation, it seems rational to choose HSV because it is familiar to many investigators and describes the colors in terms (hue, saturation, and value = brightness) easily accepted by naïve observers.

The cylindrical scheme of HSV color space presented in Fig. 3B shows the top disk corresponding to maximum-intensity colors and the bottom disk corresponding to blackness/darkness. The cylindrical surface between the two circular contours contains the maximum-saturated colors (not shown in Fig. 3B) for all intensities and for all hues presented in the circularized chromaticity diagram.

HSV color space is similar to the Munsell color space or LCh (the cylindrical representation of the CIELab space), which are more familiar to many researchers of color vision.

However, being similar to the HSV in general structure, these color spaces seem to be superfluous for our purposes since, in comparison to the HSV color space, they embrace a larger palette of colors that cannot be displayed on smartphones in conditions of our experiments.

The HSV color palette is represented by a cylinder where the display gamut occupies the whole space, with hue coordinates varying from 0 to 360°. The hue coordinates of our smartphone primaries are 0/360° for red, 120° for green, and 240° for blue. In the angular representation of the Munsell color palette, the hues of the stimuli generated on the smartphones could correspond to the ambiguous values related to both radiation and coloration. The Munsell color coordinate system does not seem to be optimal for describing radiation: it was initially developed for object colorations and later adapted for radiation. As a result, the Munsell cylindrical hue coordinate range of 38–77 corresponds to both orange (self-luminous objects) and brown (object colorations) colors, etc.

In fact, all the widespread color coordinate systems describe properties of foveal vision and only differ in their convenience for different tasks. Our task is to describe properties of the peripheral vision for which there are as yet no generally accepted color coordinate systems, and all common foveal color coordinate systems seem to be equally not quite suitable for the accurate quantitative studies of the peripheral color vision. However, like HSV, some of them are sufficient for a pilot characterization of the human color perception changes with increasing stimulus eccentricity.

General information on the smartphone models employed

In a majority of our color matching experiments, two Samsung Galaxy S8 smartphones with an AMOLED (active-matrix organic light-emitting diode) screen were employed. At the beginning of the investigation, another pair of smartphones, the Samsung Galaxy S6 with an AMOLED screen, was used (see Table 1).

We chose the smartphones with OLED screens (not LCD) because they have excellent contrast ratios and can provide high brightness and a rich gamut.

Table 1 Details of the smartphone models employed in the present study

Model	Display type	Screen resolution (pixels)	Pixels per inch	Released
Galaxy S6	Super AMOLED	2560×1440	576	2015
Galaxy S8	Super AMOLED	2560×1440	568	2017

Spectral characteristics of the smartphone primaries

It is apparent that, ideally, for accurate matching of central and peripheral stimuli, the test and reference smartphones should have identical spectral characteristics of their R, G, and B primaries. Figure 4 shows the two sets of RGB spectra for our test and reference smartphones of the two Samsung models—Galaxy S6 and Galaxy S8. All spectral characteristics were obtained with the X-Rite Eye One (i1) spectrophotometer. The measurements were carried out taking into account the period necessary for stabilization of the smartphone characteristics after its switching on. The duration of this period was assessed in advance and did not exceed 5 min.

As one can see from Fig. 4, there were small differences both between the smartphone models (S6 and S8) and between the two devices (test and reference) of the same model. All corresponding curves appeared to be similar but not quite identical. Comparing the differences between spectral characteristics of the primaries in the test–reference pairs of the S6 and S8 models, it is easy to see that S8 has some advantages, since the conformity of the curves in the pairs of its red and green primaries is better (at least as concerns the proximity of their peaks).

Unfortunately, the technical imperfectness could not be eliminated. Therefore, it was important to evaluate the influence of the described differences on the results of ACM. For this purpose, we performed the same series of measurements interchanging test and reference smartphones. The data obtained in these comparative experiments are presented in the Supplement.

Calibration of the smartphones before the color matching

Interpretation of the ACM experimental data requires some supplementary information about the smartphone calibration and specific details of the matching procedures. Calibration procedures included (1) setting each smartphone luminance at the chosen level for white stimulus; (2) measuring physical luminance, L, for the three color primaries displayed on the test and reference smartphones at different luminance levels, L_{sm}, expressed in 8-bit 256 RGB values; and (3) finding the relationship between the brightness parameter V (varying from 0 to 1) of the reference stimulus and the test stimulus luminance L_{sm} (in 8-bit 256 RGB values).

All photometric procedures were performed with the Gossen MAVO-MONITOR luminance meter. The luminance of each smartphone "white" (R = G = B = 255) was set using the "Brightness adjuster" Android application by K. Shimokura at a level of 400 cd/m^2 under photometric control. This level was chosen to enable sufficiently bright test stimuli to be presented within the zone of comfort for

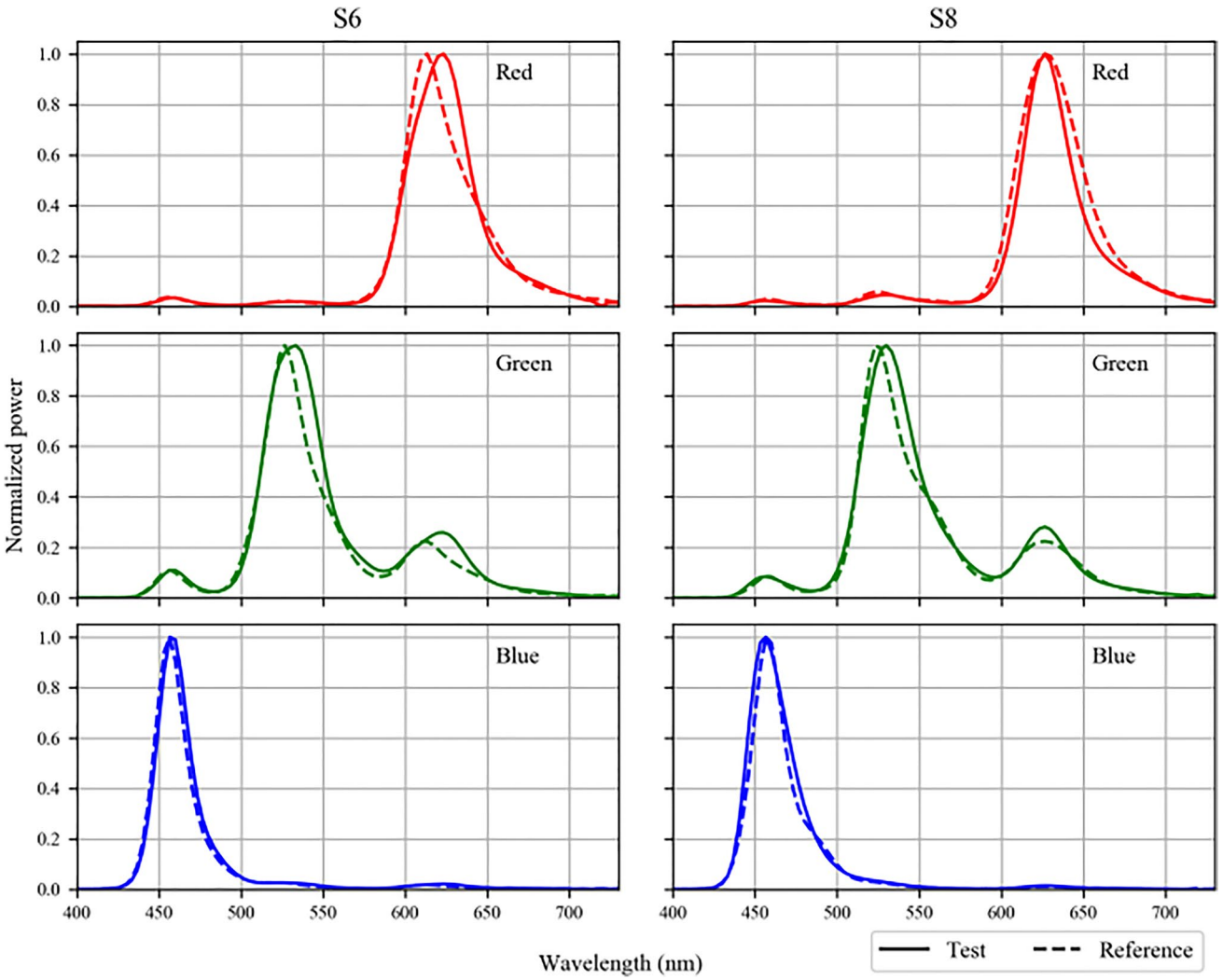

Fig. 4 Spectral characteristics of the R, G, and B primaries for the test–reference pairs of Samsung Galaxy S6 and S8 smartphones used in the experiments. Solid lines correspond to the central reference smartphone, dashed lines — to the peripheral test smartphone

human visual perception but not too close to the very highest limit (500 cd/m^2) of the devices employed.

The relationships between L_{sm} in 8-bit RGB values and the photometric data of L measurements are shown in Fig. 5. The curves corresponding to the test and reference smartphones (solid and dashed lines) appeared to be practically identical.

To estimate the smartphone's display gamma, we used manual fitting and got gamma = 2.4. Usually, in colorimetric measurements with computer displays, one sets gamma to 1, getting linear dependence of luminance on pixel value (ranging from 0 to 255 in 8-bit presentation of colors). But there are no easy ways to change display gamma in Android 9 used in our Samsung Galaxy S8 smartphones.

We also performed partial display characterization (Brainard et al., 2002) of one the smartphones used in our experiments (test smartphone). We checked luminance additivity and found that display behaved in a sub-additive manner (Toscani et al., 2019), the deviation from additivity assumption being about 15%. Channel constancy appeared to be rather good. The assessment of the ambient light effect on the stimulus spectra ("Flare") in our experimental room has shown that ambient light correction is not needed for L_{sm} equal to 50 or greater. All these data (including spectral measurements, and CIE xyY color model xy coordinates of the smartphone primaries) are accessible on https://github.com/abelokopytov/spot/raw/master/DisplayCharacterization.xlsx.

Additional information characterizing the smartphone properties relevant to our experiments is given in the Supplement: effect of the temperature on the luminance of each primary; effect of the reference stimulus temporal mode (flickering vs. stationary) on the results of matching; and effect of interchanging the test and reference smartphones.

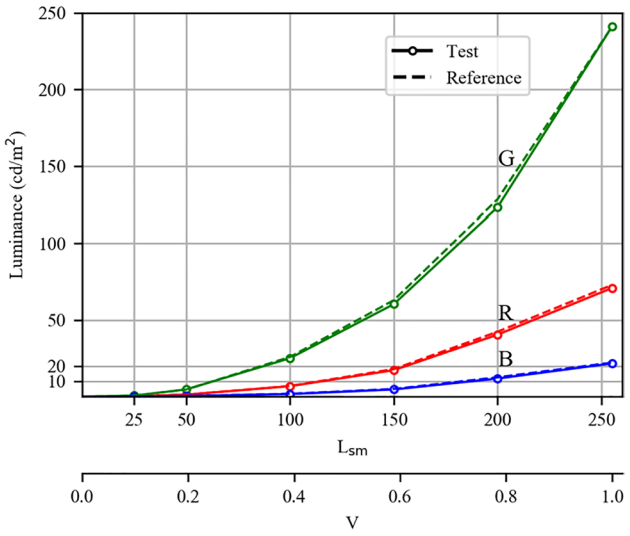

Fig. 5 Relationships between L_{sm} (in 8-bit RGB values), value V (in HSV color space), and photometric luminance L for the three primaries of the test and reference smartphones (solid and dashed lines, respectively)

Participants

Participants were eight volunteers (three female, five male), aged 19–46 years. According to the results of a standard clinical examination (assessment of refraction, accommodation, visual resolution, and color discrimination), all participants had normal visual acuity and normal trichromatic color vision assessed by CAD (color assessment and diagnosis) test by City Occupational Ltd. As concerned color matching, three participants were experienced while the other five were naïve observers. Our investigation included two stages: (1) a preliminary stage consisting of short experimental sessions aimed at selecting suitable stimulus parameters, refining the experimental protocol, and obtaining initial tentative results; and (2) the main stage aimed at collecting data sufficient for thorough analysis and reliable conclusions. All eight observers participated in the preliminary stage, providing an opportunity to develop reasonable experimental protocols and to assess inter-subject variability in responses. However, only half of the observers could participate in the main experiments, which were rather tiresome and of substantial duration.

The study was carried out in accordance with the Declaration of Helsinki (2013). Prior to testing, written informed consent was obtained from each participant. The experimental procedure was approved by the ethics board of the Institute for Information Transmission Problems.

Stimuli

The peripheral test stimuli were uniform colored spots of 4 cm diameter (about 7°) turning on/off every 1.5 s. The reference stimuli were of the same size as the test ones; however, for ease of matching, the reference stimuli did not turn on/off, since these stimuli had to be permanently adjusted.

The size of the test stimuli was large enough to make them well seen at the periphery. Low-frequency flicker was used to provide comfortable conditions for prolonged observation of the test stimuli at the far periphery, taking into consideration the well-known Troxler effect—fading of stationary peripheral stimuli in conditions of gaze fixation on the center of the VF (Troxler, 1804). The duration of the "on" and "off" phases was chosen so as to (1) prevent such fading, (2) provide suitable temporal conditions for the matching procedure, and (3) avoid the development of noticeable afterimages arising after the stimulus offset in the cases of high stimulus luminance and long duration. Performing several preliminary experiments with "on" and "off" phase durations of 1.0, 1.5, and 2.0 s for comparison, we became convinced that the results were similar, but the presentation mode of 1.5/1.5 s seemed to be somewhat more comfortable for our observers.

In the main series of our experiments, the color of each test stimulus corresponded to one or another of the smartphone primaries—R, G, or B (their spectral curves are shown in Figs. 1B and 4). The luminance of the test stimuli (L_{sm}) was set in 8-bit 256 RGB values: $25 \le R \le 255$, $G = 0$, $B = 0$ for the red stimuli; $R = 0$, $25 \le G \le 255$, $B = 0$ for the green ones; $R = 0$, $G = 0$, $25 \le B \le 255$ for the blue ones. During the course of each experimental session, six levels of L_{sm} were used for red, green, and blue stimuli: 25; 50; 100, 150, 200, and 255.

The perceived color of the peripheral test stimulus was estimated by properly adjusting the central reference stimulus and was expressed in HSV color coordinates. In this notation, all the test stimuli should ideally have the following perceived hue values H in an angular dimension: $H(R) = 0/360$; $H(G) = 120$; $H(B) = 240$. The range for the intensity parameter V (the value characterizing brightness) was from 0 to 1.0. As concerned the saturation S, the possible range is also from 0 to 1; ideally, for all our test stimuli, this parameter should always be maximal ($S = 1$), since each test stimulus was a pure smartphone primary. At the same time, the spectral curves shown in Fig. 2 indicate that green stimuli could be perceived as somewhat less saturated than red and blue ones because of the larger additional lateral peaks.

The physical levels of the stimulus luminance (L in cd/m^2) corresponding to each L_{sm} value could be determined using the calibration curves presented in Fig. 5.

The additional series of experiments was devoted to a more thorough investigation of the peripheral stimuli saturation. In this series we used not only the smartphone's primaries, but also less saturated test stimuli. The intensity parameter V was fixed at the level of 0.6.

The following eccentricities along the horizontal meridian in the temporal half of the VF were chosen for detailed measurements: 0°, 25°, 40°, 60°, 80°, and 95°. Unequal intervals at the beginning and end of the eccentricity range were used to avoid areas near the regions corresponding to the blind spot and the margin of the retina, the ora serrata.

Procedure

The stimuli were presented in a dimly lit room with illumination of 5 lx. At the beginning of each measurement session, the observers were given 5 min to adapt to this level of ambient light and to familiarize themselves with the equipment. The experiments were carried out in conditions of monocular viewing and keeping the gaze on the central reference stimulus. During the measurements, the participant was seated in such a way that his/her right eye visual axis was directed to the reference stimulus at the center of the perimetric arc. The left eye was covered with an opaque patch. The observer's head was supported by a chin rest. The peripheral test stimulus, displayed on the smartphone at variable eccentricity, and the reference stimulus displayed on the second smartphone located centrally were observed simultaneously. Since the reference stimulus had the same relatively large size as the test one (7°), it would be not quite correct to use the term "foveal fixation". According to a widely accepted view, the diameter of the foveal area is about 5° (unfortunately, there are no reliable data on inter-subject variability of this parameter); therefore, it is more proper to say that our observers were examined under conditions of central fixation and that the variation in the eccentricity of the peripheral test stimulus was greater than with the use of a fixation point at the very center of the VF.

The participant's task was to make the appearance of the central reference stimulus as similar as possible to the appearance of the peripheral test stimulus, adjusting the hue (H), saturation (S), and brightness (V) of the reference stimulus. The participants could easily control the parameters of the reference stimulus using a mouse connected to the reference smartphone. To change the hue and saturation of the reference stimulus, the participant had to move the mouse left–right and forward–backward, respectively; brightness was adjusted by turning the wheel. The time given for matching was not limited. Each trial could take several seconds or one-two dozens of seconds depending on the participant's capabilities and test stimulus parameters. Once a satisfactory match was reached, the participant pressed the button on the mouse to save the result. The recorded HSV values were displayed on the reference smartphone after each completed trial and disappeared before the next trial.

Most participants were tested over a period of 2–5 days since the final standard protocol of our main experiments included too many measurements to be completed in one working day. Participants had to perform matching for three primaries (R, G, B) and obtain three estimates (H, S, and V) at each of six luminance levels (25, 50, 100, 150, 200, and 255 in RGB scale) for the test stimuli presented at six eccentricities (0°, 25°, 40°, 60°, 80°, and 95° on the horizontal meridian of the temporal VF). In the main series of experiments, the measurements were performed five times; the final dataset for each participant contained at least $3 \times 3 \times 6 \times 6 \times 5 = 1620$ values. In the additional series of experiments, the measurements were performed three times.

Results

Since our main purpose was to consider the possibilities and the specifics of the proposed technique, we focused our attention on encompassing the whole range of eccentricities and obtaining comprehensive data on the general features of peripheral color vision.

Presenting color test stimuli at the periphery (temporal VF, 25°–95°), we have found that, in the whole range of the eccentricities used, the perceived peripheral stimuli were clear and vivid. At the same time, it is necessary to mention an important peculiarity of the colors perceived at the periphery: in most cases, the observers could choose the central stimulus most similar to the peripheral test stimulus; however, the task of setting a completely identical central stimulus on the reference smartphone was not always feasible even though the response time was not limited. For this reason, each participant was instructed to do his/her best but not to be too anxious if the desired perfect matching appeared to be unattainable.

From the description of our matching method, it is evident that in each measurement, all three quantitative estimates of the perceived peripheral color—H, S, and V—were obtained simultaneously. These estimates were displayed at the reference smartphone just after the participant had chosen the most suitable central stimulus and pressed the mouse button. However, in order to simplify the description and interpretation of the experimental data, H, S, and V estimates will be considered separately.

Perceived hue of the peripheral stimuli, H-estimates

The data characterizing the dependence of the H-estimate on the test stimulus luminance L_{sm} and eccentricity are shown in Fig. 6. This figure contains H-estimates obtained in four participants for five levels of the smartphone luminance L_{sm}

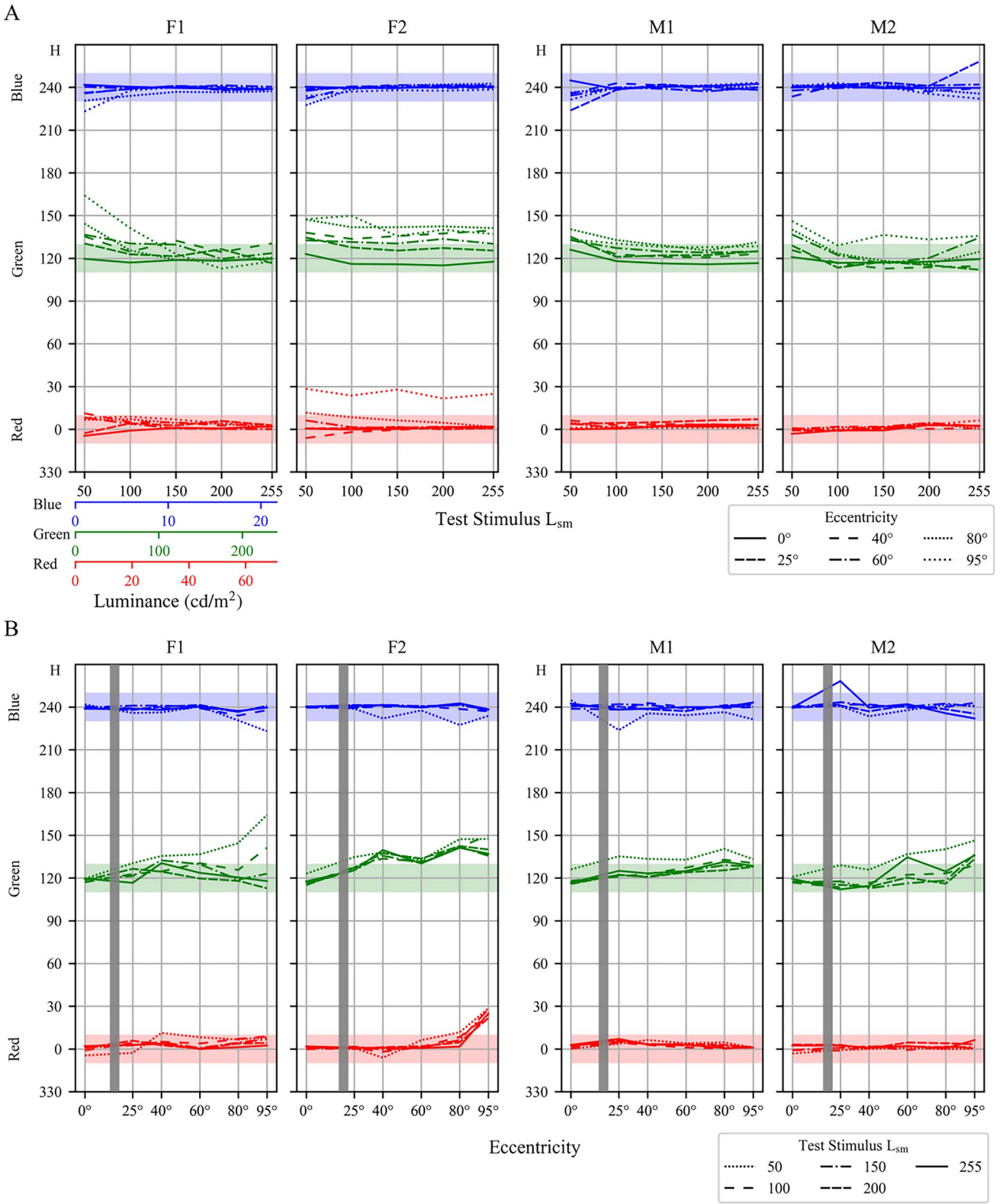

Fig. 6 Perception of hue (H) at various luminance levels (L_{sm}) and eccentricities of the peripheral test stimuli. Data for four participants—two females (F1 and F2) and two males (M1 and M2)—are presented to illustrate inter-individual differences. **A** H as a function of L_{sm} for various eccentricities. **B** H as a function of eccentricity for various L_{sm}. Gray bars indicate the angles corresponding to the blind spot in the retina of each participant

(50, 100, 150, 200, and 255) and six eccentricities (0°, 25°, 40°, 60°, 80°, and 95°). At the lowest luminance used in the experiment, $L_{sm} = 25$, the participants were not always sure in their matches, and we discarded these measurements.

Figure 6A presents the curves showing the dependence of H on L_{sm} for the six eccentricities. As one can conclude from this figure, in the case of the blue peripheral stimulus, the H-estimates were close to the true value of the central ones (240) up to the largest eccentricity of 95° in all four participants; all individual lowest L_{sm} levels providing good similarity did not exceed 100.

In the case of the red stimuli, the peripheral H-estimates were close to the central ones (0/360) up to the largest eccentricity of 95° in three of four participants (F1, M1, M2); as in the case of blue stimuli, their individual lowest L_{sm} levels providing good similarity did not exceed 100. In the participant F2, at eccentricity of 95°, the same red stimuli were perceived as orange ones, with H-estimates from 22 to 28, independently of L_{sm}. In conditions of our experiments, this participant could only perceive the peripheral red stimuli as pure red spots up to eccentricity of about 60°. It is worth noting that, with increasing L_{sm}, in participant F3 (not included in Fig. 6), at eccentricity of 95°, H-estimates changed from $H = 110$ (yellow-green) to $H = 0$ (pure red).

In the case of the green test stimuli, at eccentricity of 95°, H-estimates of two participants (F2 and M2) did not approach the "true green" value ($H = 120$) with increasing luminance even at the highest L_{sm} levels. In F2, the perceived colors remained somewhat bluish (130÷140) with increasing intensity even at the lower eccentricities.

Certain features of the perceived color changes at the periphery of the VF are better seen in Fig. 6B, showing the dependence of H on eccentricity for five values of L_{sm}. Most dotted lines corresponding to the lower levels of luminance, $L_{sm} = 50$, demonstrate significant deviations of the perceived hue at the periphery from the central one. In some cases these deviations increased with eccentricity: for instance, see H-estimates for green test stimuli in subjects F1, F2, and M2. However, in other cases, the curves were less monotonic, evidently because of the errors, indicating an insufficient number of trials and/or significant influence of certain individual factors besides eccentricity.

Brightness of the peripheral stimuli, V-estimates

The brightness (V-estimate) of the peripheral stimulus was typically higher than that of the central one, the difference being maximal in the eccentricity range of 40–80°. The combined data of four participants in Fig. 7 illustrate these results, showing the dependence of the brightness estimates V on the L_{sm} level at various eccentricities (Fig. 7A) and the dependence of the brightness estimates V on the eccentricity for different L_{sm} levels (Fig. 7B). The curves of Fig. 7A indicate that, at the periphery, in contrast to the central region, the dependence of V on the L_{sm} could be essentially nonlinear. This feature is better expressed around the eccentricity of 60°.

As one can conclude from Fig. 7A, the brightness of the peripheral red, green, and blue stimuli was higher around 60° than at 0° for all participants and for all levels of L_{sm} exceeding $L_{sm} = 25$. Note that some curves in Fig. 7 are marked with stars and are not completed. The stars correspond to the responses "> 1" marking the L_{sm} levels (Fig. 7A) or eccentricities (Fig. 7B) over which the exact matching in V was impossible. In such cases, the limiting value of the reference central stimulus, $V = 1$, appeared to be "too small" to reflect the brightness of the peripheral test stimulus, and we could not obtain any quantitative measure of its superiority over the central stimulus.

Accordingly, in Fig. 7A, most curves obtained for the peripheral test stimuli approached the brightness level $V = 1$ at the L_{sm} values essentially lower than 255, the value which should theoretically correspond to $V = 1$ according to the color perception model taken as a basis in the HSV color coordinate system for trichromatic human central color vision. Moreover, in most cases, the data corresponding to the higher L_{sm} level could not be presented in Fig. 7 since the matching in V was impossible: the participant reported that the peripheral test stimulus looked brighter, or even much brighter, than the brightest central stimulus that could be generated (corresponding to $V = 1$).

The graphs of Fig. 7B enable a better understanding of the general dependence of the brightness estimates on eccentricity. More detailed analysis of Fig. 7B reveals significant inter-subject variability in the peripheral perception of brightness. In participant F2, the data for R-, G-, and B-stimuli were similar to each other, and the maximal V-values were obtained at eccentricity of 60°. At the extreme periphery of 95°, most V-estimates were noticeably higher than the estimates of central stimuli. In participant F1, the data for R-, G-, and B-stimuli appeared to be essentially different; the stimulus eccentricities for the largest V-values varied in the range of 40°–80°. The difference between V-values at the extreme periphery and in the central region was small barring the cases of the two upper curves for the blue test stimuli. The data for participants M1 and M2 had their own peculiarities, but also demonstrated a general increase in V-values with increasing eccentricity to 40°–80° and a decrease after reaching the maximum value.

One could propose various explanations for the described general shape of the curves and their inter-individual variability. However, it seems premature to do this now, taking into account the limited amount of the data obtained, which is insufficient for thorough analysis although sufficient for certain definite conclusions. One of the evident conclusions is the need to assess the contribution of rods and maybe of

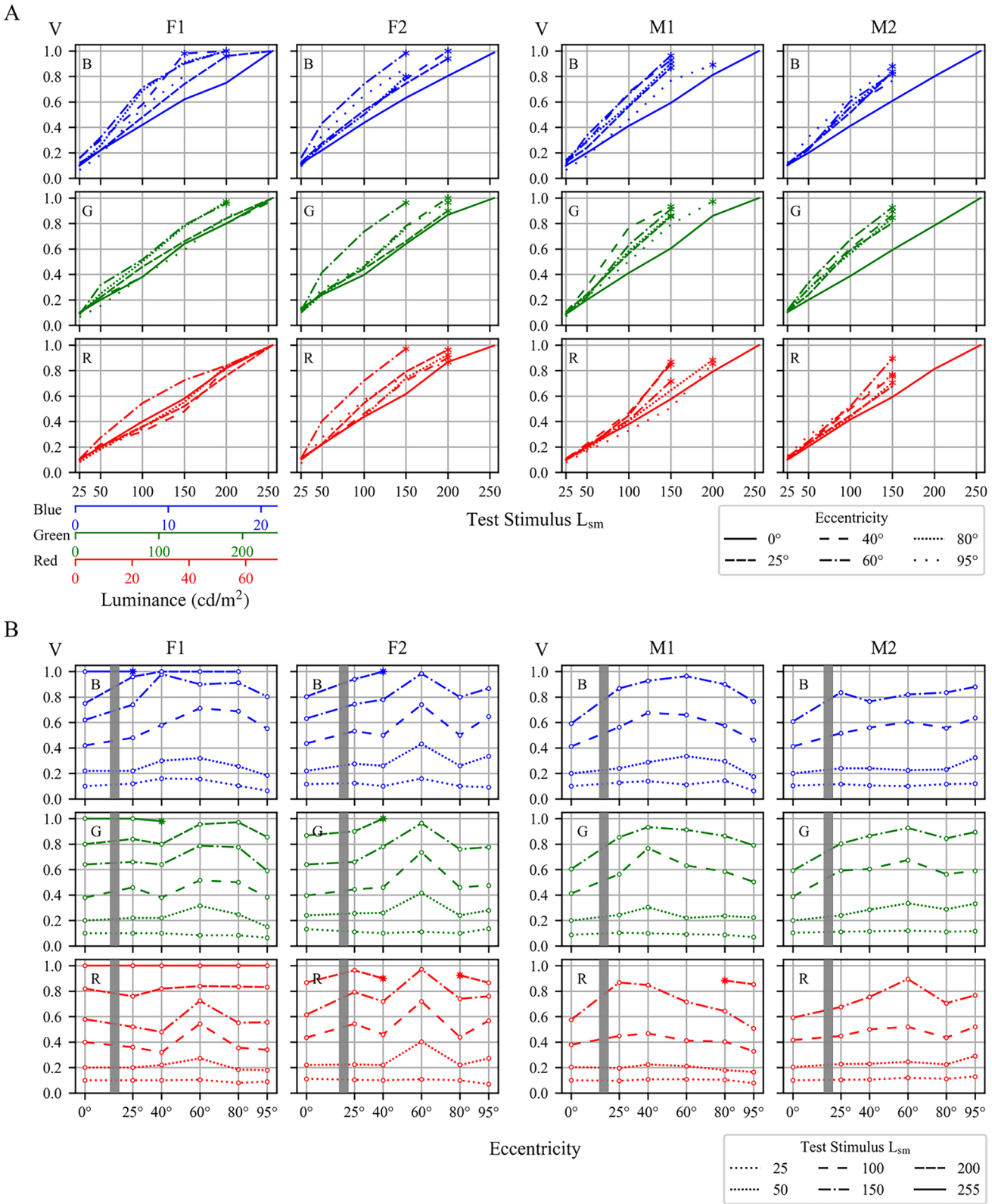

Fig. 7 Brightness (V) as a function of stimulus luminance (L_{sm}) and eccentricity. The data for four participants, two females (F1 and F2) and two males (M1 and M2). **A** V as a function of L_{sm} for various eccentricities. **B** V as a function of eccentricity for various L_{sm}. Gray bars indicate the angles corresponding to the blind spot in the retina of each participant. The stars indicate the margins of the super-brightness ranges

ipRGCs to color perception, since the HSV color system appeared to be inappropriate for quantitative representation of the whole variety of the perceived colors.

Saturation of the peripheral stimuli, S-estimates

The data on saturation of the peripheral stimuli obtained in the main series of our experiments are presented in Fig. 8.

As was indicated in Methods, in this series our color test stimuli always corresponded to the RGB primaries of the smartphones used in the experiments. Thus, the spectra of the stimuli were almost the same for all stimulus intensities, and it was natural to expect that all estimates of saturation should be equal or close to the value S = 1 prescribed to pure R, G, and B primaries, independently of their luminance.

In most cases, the data obtained for R- and B-stimuli at lower values of L_{sm} (< 150) and eccentricities (< 60°) appeared to be close to this expectation: the preponderance of S-estimates was between 0.95 and 1 (Fig. 8A). Because of such a narrow range, many curves appeared to be very near each other or even fused.

However, at the far periphery, certain specific difficulties arose with the saturation of the bright test stimuli (L_{sm} >150). Such stimuli could look more saturated than the central reference ones with S = 1, thus making matching in S forbidden since, in the HSV color space, S > 1 is inadmissible. In Fig. 8, such cases are marked with stars (*) on corresponding curves. Since many curves are superimposed, the implied eccentricities (Fig. 8A) and L_{sm} levels (Fig. 8B) are indicated near the curves.

The situation with G-stimuli was more complicated, supposedly because of the lateral peaks in the spectrum of the smartphone's G-primary. On average, in the case of green stimuli, the correspondence between the best matched peripheral and central S-estimates was worse than in the cases of R- and B-stimuli.

It was also observed that when the participants perceived the peripheral stimulus as "superior" to the central one with S = 1 and V = 1, in some cases they could not separate contributions of saturation and brightness to this superiority. In such situations, the uncertain estimates "> 1" could be prescribed to V, S, or both. One could suppose that our participants needed some training in the assessment of saturation. Though their oral responses evidenced against this assumption, we are going to check it in future studies.

Since in many cases of the main experimental series the participants reported supersaturation and/or superbrightness (i.e., S = 1 and/or V = 1 were insufficient to characterize the observed high saturation and/or brightness of the peripheral stimuli), we performed additional pilot experiments with less saturated and less bright test stimuli.

In this series, we used a fixed test stimulus brightness level V = 0.6 and varied saturation of the peripheral test stimuli from S = 0.3 to S = 1.0. The results are presented in Fig. 9.

One can see that, as a rule, S-estimates for the peripheral stimuli were larger than for the foveal ones. Typically, S-estimates increased with eccentricity up to 40°–60° and decreased after reaching certain maximum values, but these dependencies demonstrated significant inter-individual variability (similar to the variability in V-estimates shown in Fig. 7), making it either senseless or premature to speak about a uniform average regularity.

The exceeding of the peripheral S-estimates over the foveal ones was more pronounced for the test stimulus saturation levels of 0.4–0.6. For less saturated test stimuli, the effect was diminished or absent. As an example, one can compare the R-graphs for the test stimulus saturation of 0.3: in participant F2, S-estimates were practically independent of eccentricity, and in participant M2, S-estimates even decreased, while in participant F1, all the peripheral S-estimates were larger than the foveal one.

It is evident that a larger dataset is needed for more adequate and convincing conclusions; however, at present, collection of such a dataset is problematic because of the pandemic restrictions. We believe that despite the limited amount of data collected, there is no doubt that certain stimuli at the periphery could be perceived as more saturated than the identical ones at the fovea.

Discussion

Based on the results, we can conclude that the developed perimetric setup with two smartphones for displaying peripheral test and central reference stimuli proved to be suitable for comparing and matching the appearance of color stimuli presented peripherally and centrally.

We would like to note that, in the pilot series of experiments reported here, not all commonly employed means were used that otherwise would have allowed us to improve the precision of measurements. In particular, in an attempt to reduce the discomfort and fatigue usually experienced by observers in a typical study of peripheral vision, we did not apply bite bars, pupil dilatation, the Maxwellian view, or prolonged, many-stage adaptation procedures out of concern for the participants (for example, see a description of inconveniences caused by maintaining the state of the Maxwellian view during experiments in Neitz and Jacobs (1990)).

Furthermore, we used a modified ACM procedure where we forwent the central reference stimulus flickering to ease its adjustment; thus, the peripheral test stimulus was turned on/off every 1.5 s, while the central reference stimulus was presented without flickering. To ensure that

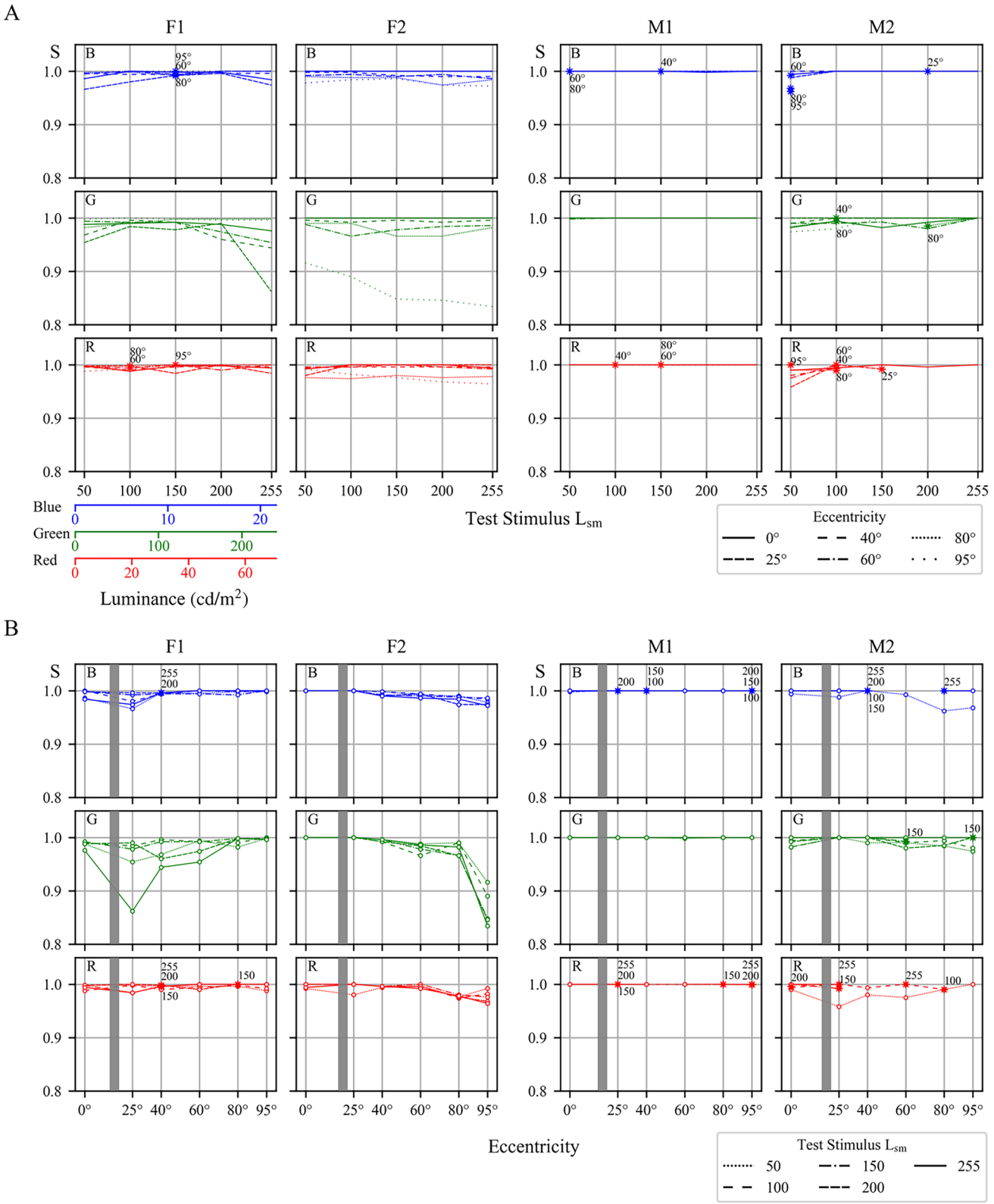

Fig. 8 Saturation (S) as a function of stimulus luminance (L_{sm}) and eccentricity. The data for four participants, two females (F1 and F2) and two males (M1 and M2). **A** S as a function of L_{sm} for various eccentricities; **B** S as a function of eccentricity for various L_{sm}. Gray bars indicate the angles corresponding to the blind spot in the retina of each participant. The stars indicate the cases of supersaturation

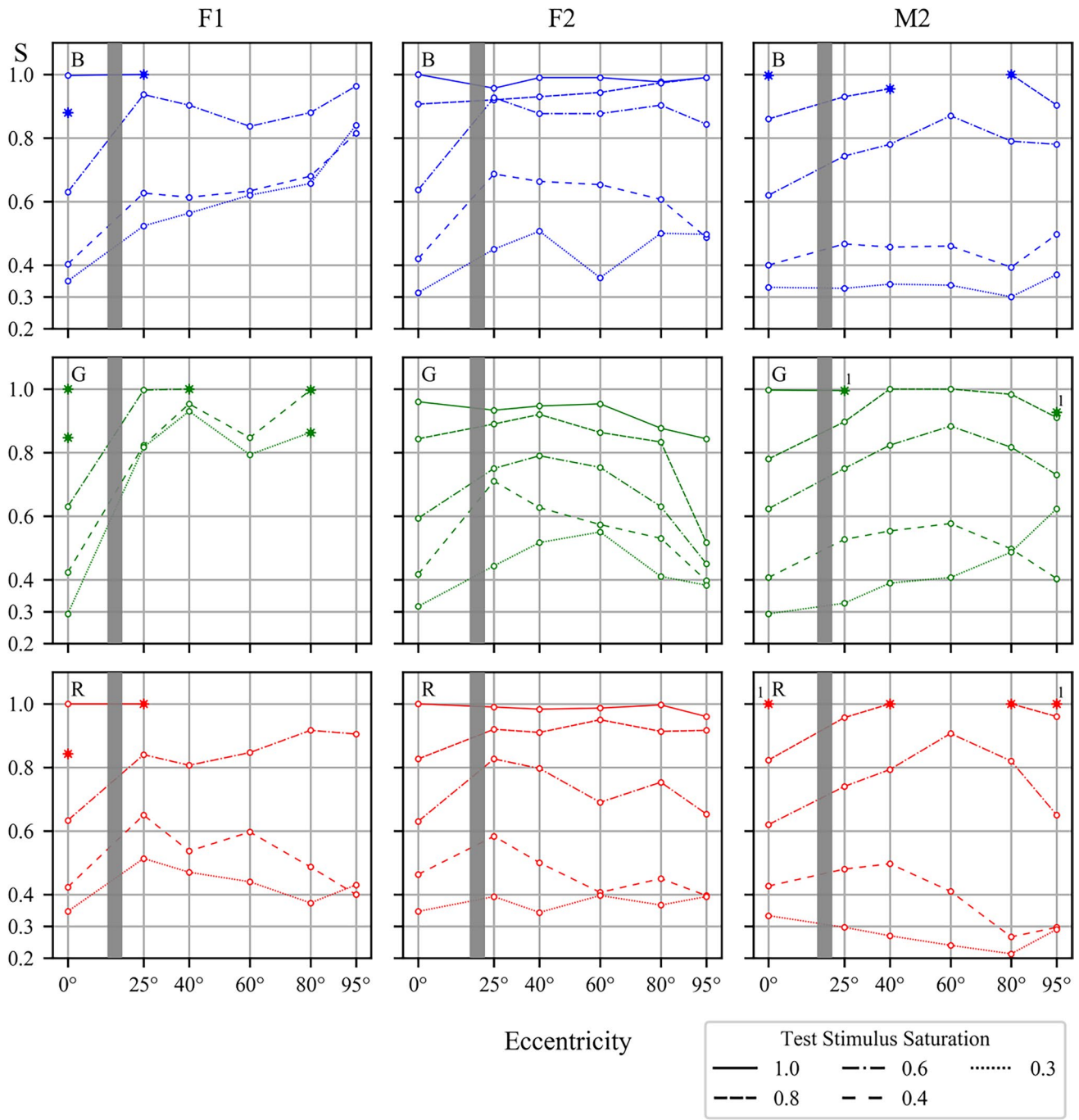

Fig. 9 Saturation (S) of the peripheral stimulus as a function of its eccentricity for several levels of the test saturation (0.3–1.0) in the cases of V = 0.6 and H = 0 (R graphs), 120 (G graphs), and 240 (B graphs). The data for the three participants: two females (F1 and F2) and one male (M2). Each point represents the average of the three ACMs. Gray bars indicate the angles corresponding to the blind spot in the retina of each participant. The stars indicate the cases of supersaturation

this modification of the experimental procedure did not affect the outcomes of the ACM, we conducted control experiments with and without flickering of the central reference stimulus. As Figure S3 (Supplement) shows, the results from the two conditions did not differ significantly.

Despite the simplifications and modifications mentioned above, the resulting accuracy of the measurements appeared to be satisfactory for making certain conclusions. Our data provided evidence that the proposed ACM technique could be employed over a range of eccentricities up to 95°, i.e., to

the extreme VF (and retinal) periphery. Thus, we extended the findings of the psychophysical studies showing that deterioration of color vision with increasing eccentricity could be compensated by increasing the size and/or luminosity of the peripheral test stimuli (Noorlander et al., 1983; van Esch et al., 1984; Abramov et al., 1991; Murray et al., 2006; Tyler, 2015, 2016; etc.). Further, we demonstrated significant inter-individual differences in color perception at the periphery. Experimental data obtained for a wide range of eccentricities and for several observers enabled us to gain insight into the causes of certain peculiarities and seemingly contradictory outcomes of some experimental investigations (e.g., Abramov & Gordon, 1977; Murray et al., 2012; Opper et al., 2014; Stabell & Stabell, 1976) concerning the eccentricity-dependent color appearance of the stimuli (constancy vs. changes in the perceived hue; enhancement vs. diminishing of saturation; the phenomena of supersaturation, etc.).

We are cognizant of limitations of the proposed technique; however, we hope that its main advantages—simplicity, affordability, and accessibility—could attract the attention of behavioral scientists and encourage willing researchers to contribute to the investigations of color stimulus perception at the VF periphery.

Although the literature on color vision is vast, the majority of books and articles address central vision only. The studies on peripheral color vision are scarce; many of these were carried out after a long training of the observers (e.g., Abramov & Gordon, 1977; Neitz & Jacobs, 1990). In many cases, only the authors could meet the challenges, i.e., master the experimental procedures and endure the experiment duration (e.g., Moreland & Cruz, 1959; Nerger et al., 1995; Opper et al., 2014; Stabell & Stabell, 1979, 1982a, 1982b, 1984, 1996). In contrast, in our experiments, most of the observers were able to perform all required measurements after a brief explanation and several short trials. This is encouraging for the data collection process.

Regarding the employment of smartphones and miniature computer devices for color vision research, recent literature shows a positive tendency both in laboratory studies and in elaboration of color vision tests for field investigations (see Barbur et al., 2020; Bodduluri et al., 2017, 2018; Dain et al., 2016; Pyayt, 2020). It is well known that one of the barriers to effective application of such devices is significant variability of colorimetric characteristics between devices, as well as instability of colorimetric parameters, which necessitates proper selection and calibration of the devices. Luckily, in this respect, the situation is improving quite rapidly: as a rule, each new model demonstrates better colorimetric quality.

Finally, it is necessary to mention some important theoretical aspects of color vision study at the periphery of the VF projecting onto the periphery of the retina. The structural heterogeneity of the retina, addressed in the Introduction, is apparently reflected in its functional heterogeneity. It seems reasonable to suppose that retinal regions of different eccentricity are designed for both common visual functions and for location-specific functions. The task of color identification is common for all locations at the VF. This implies that, comparing the central and peripheral vision performance in the same visual task, one could potentially reveal either a functional similarity, or superiority of one over the other.

In general, different tasks require specific experimental paradigms and procedures. Because of novel data on the contribution of rods to chromatic discrimination (e.g., Buck, 2001; Cao et al., 2008) and ipRGCs to color perception (e.g., Cao & Barrionuevo, 2015; Schroeder et al., 2018; Spitschan, 2019; Zele et al., 2018), it becomes apparent that, instead of conventional three-dimensional or four-dimensional color spaces (Brill, 1990; Polymeropoulos et al., 2011; Smith & Pokorny, 2003; Trezona, 1970, 1973, 1974), a more appropriate model would require a five-dimensional color space to describe the full variety of colors perceived under different experimental conditions (ambient light level, range of eccentricities, stimulus parameters). Moreover, an investigation of various neuronal mechanisms of color perception that combine inputs from the four photoreceptor types and ipRGCs could require fundamentally more complicated models than those developed until now. For example, even in 2007, Solomon and Lennie in their review "The machinery of colour vision" wrote: "…modern work has drawn attention to unexpected complexities of early organization … We describe, in the retina and in the lateral geniculate nucleus, many more pathways for colour signals than seemed possible only 15 years ago" (Solomon & Lennie, 2007, p. 276).

It is, however, premature to expect rapid success in the development of adequate general information on both the machinery underlying the visual mechanisms (fine morphology and neurophysiology of the human retina and the visual brain centers) and behavioral responses (psychophysical and psychological data) characterizing color perception in natural situations. The complexity and heterogeneity of the human retinal structure and functions are still far from being studied in all details, or fully understood. Most psychophysical data have been obtained in specific artificial experimental conditions of eye fixation suppressing the peripheral mechanisms, which makes it problematic to puzzle out a general scheme of the peripheral color vision. In our view, further development of psychophysical experiments would require a greater variety of designs that would be more easily put into practice and enable capturing color vision phenomena under natural-viewing, ecologically valid conditions. Among various contemporary methods that are promising in this respect, we consider a technique of immersion in dynamic virtual reality (e.g., Cohen et al., 2020) and simulating central scotoma by means of contact lenses (Almutleb et al., 2018; Iomdina et al., 2020; Rozhkova, Iomdina, et al., 2019b) and

other accessible methods akin to the method described in the present paper. We are aware, though, that as they are relatively immature, such methods require further assessment and fine-tuning.

Supplementary Information The online version contains supplementary material available at https://doi.org/10.3758/s13428-021-01783-3.

Acknowledgements We are greatly indebted to Prof. Galina Paramei for critical reading of our manuscript and helpful discussions, and to our colleagues, Prof. Nadezhda Vasilyeva and Anna Kazakova, for their assistance in many of our experiments.

Funding Research was partially funded by Russian Foundation for Basic Research (19-015-00396A).

Declarations

Conflicts of interest The authors declare no conflicts of interest.

References

Abramov, I., & Gordon, J. (1977). Color vision in the peripheral retina. I. Spectral sensitivity. *Journal of the Optical Society of America*, *67*(2), 195-202. https://doi.org/10.1364/JOSA.67.000195

Abramov, I., Gordon, J., & Chan, H. (1991). Color appearance in the peripheral retina: effects of stimulus size. *Journal of the Optical Society of America A*, *8*(2), 404-414.

Allen, A. E., Martial, F. P., & Lucas, R. J. (2019). Form vision from melanopsin in humans. *Nature Communications*, *10*(1), 1-10. https://doi.org/10.1364/JOSAA.8.000404

Almutleb, E. S., Bradley, A., Jedlicka, J. & Hassan, S. E. (2018) Simulation of central scotoma using contact lenses with an opaque centre. *Ophthalmic and Physiological Optics, 38* (1), 76-87. https://doi.org/10.1111/opo.12422

Ambler, B. A. (1974). Hue discrimination in peripheral vision under conditions of dark and light adaptation. *Perception & Psychophysics*, *15*(3), 586–590. https://doi.org/10.3758/BF03199306

Baraas, R. C., & Zele, A. J. (2016). Psychophysical correlates of retinal processing. In R. C. B*araas*, J. Kremers, & N. J. Marshall (Eds.), *Human Color Vision* (pp. 133-157). Springer. https://doi.org/10.1007/978-3-319-44978-4_5

Barbur, J. L., Rodriguez-Carmona, M., & Evans, B. E. (2020). Color vision assessment 3. An efficient, two-step, color assessment protocol. *Color Research & Application*, *46*(1) 33-45. https://doi.org/10.1002/col.22599

Berson, D. M., Dunn, F. A., & Takao, M. (2002). Phototransduction by retinal ganglion cells that set the circadian clock. *Science*, *295*(5557), 1070-1073. https://doi.org/10.1126/science.1067262

Bodduluri, L., Boon, M. Y., & Dain, S. J. (2017). Evaluation of tablet computers for visual function assessment. *Behavior Research Methods*, *49*(2), 548-558. https://doi.org/10.3758/s13428-016-0725-1

Bodduluri, L., Boon, M. Y., Ryan, M., & Dain, S. J. (2018). Normative values for a tablet computer-based application to assess chromatic contrast sensitivity. *Behavior Research Methods*, *50*(2), 673-683. https://doi.org/10.3758/s13428-017-0893-7

Brainard, D. H., Pelli, D. G. and Robson, T. (2002). Display Characterization. In: J. P. Hornak (ed.), *Encyclopedia of Imaging Science and Technology*. https://doi.org/10.1002/0471443395.img011

Brill, M. H. (1990). Mesopic color matching: some theoretical issues. *Journal of the Optical Society of America A*, *7*(10), 2048-2051. https://doi.org/10.1364/JOSAA.7.002048

Buck, S. L. (2001). What is the hue of rod vision? *Color Research & Application*, *26*(S1), S57-S59. https://doi.org/10.1002/1520-6378(2001)26:1+<::AID-COL13>3.0.CO;2-J

Cao, D., & Barrionuevo, P. A. (2015). The importance of intrinsically photosensitive retinal ganglion cells and implications for lighting design. *Journal of Solid State Lighting*, *2*(1), 10. https://doi.org/10.1186/s40539-015-0030-0

Cao, D., Pokorny, J., Smith, V. C., & Zele, A. J. (2008). Rod contributions to color perception: linear with rod contrast. *Vision research, 48*(26), 2586-2592. https://doi.org/10.1016/j.visres.2008.05.001

Cohen, M. A., Botch, T. L., & Robertson, C. E. (2020). The limits of color awareness during active, real-world vision. *PNAS*, *117*(24), 13821–13827. https://doi.org/10.1073/pnas.1922294117

Commission Internationale de l'Eclairage [CIE]. (2018). CIE S 026/E:2018 - CIE system for metrology of optical radiation for ipRGC-influenced responses to light. Vienna, Austria: CIE Central Bureau. https://doi.org/10.25039/S026

Curcio, C. A., Sloan, K. R., Packer, O., Hendrickson, A. E., & Kalina, R. E. (1987). Distribution of cones in human and monkey retina: individual variability and radial asymmetry. *Science*, *236*(4801), 579-582. https://doi.org/10.1126/science.3576186

Curcio, C. A., Sloan, K. R., Kalina, R. E., & Hendrickson, A. E. (1990). Human photoreceptor topography. *Journal of Comparative Neurology*, *292*(4), 497-523. https://doi.org/10.1002/cne.902920402

Dacey, D. M., Liao, H. W., Peterson, B. B., Robinson, F. R., Smith, V. C., Pokorny, J., Yau, K-W., & Gamlin, P. D. (2005). Melanopsin-expressing ganglion cells in primate retina signal colour and irradiance and project to the LGN. *Nature*, *433*(7027), 749-754. https://doi.org/10.1038/nature03387

Dain, S. J., Kwan, B., & Wong, L. (2016). Consistency of color representation in smart phones. *Journal of the Optical Society of America A*, *33*(3), A300-A305. https://doi.org/10.1364/JOSAA.3300A300

Gordon, J., & Abramov, I. (1977). Color vision in the peripheral retina. II. Hue and saturation. *Journal of the Optical Society of America*, *67*(2), 202-207. https://doi.org/10.1364/JOSA.67.000202

Graham, D. (2014, February). *Melanopsin ganglion cells: a bit of fly in the mammalian eye*. Retrieved 2020, December 28 from http://webvision.umh.es/webvision/Melanopsin.html

Graham, D., Wong, K. Y., Pattabiraman, K., & Berson, D. M. (2007). A Bit of fly in the mammalian eye. *Investigative Ophthalmology & Visual Science*, *48*(13), 2850

Greenstein, V. C., & Hood, D. C. (1981). Variations in brightness at two retinal locations. *Vision Research, 21*, 885–891. https://doi.org/10.1016/0042-6989(81)90189-9

Hannibal, J., Christiansen, A. T., Heegaard, S., Fahrenkrug, J., & Kiilgaard, J. F. (2017). Melanopsin expressing human retinal ganglion cells: Subtypes, distribution, and intraretinal connectivity. *Journal of Comparative Neurology*, *525*(8), 1934-1961. https://doi.org/10.1002/cne.24181

Hansen, T., Pracejus, L., & Gegenfurtner, K. R. (2009). Color perception in the intermediate periphery of the visual field. *Journal of Vision*, *9*(4), 26-26. https://doi.org/10.1167/9.4.26

Hattar, S., Liao, H. W., Takao, M., Berson, D. M., & Yau, K. W. (2002). Melanopsin-containing retinal ganglion cells: architecture, projections, and intrinsic photosensitivity. *Science*, *295*(5557), 1065-1070. https://doi.org/10.1126/science.1069609

Iomdina, E. N., Selina, O. M., Rozhkova, G. I., Belokopytov, A. V., & Ershov, E. I. (2020). Contact lens with implanted occluder as a tool for assessment of far peripheral vision in natural viewing conditions. *Sensornye sistemy* [Sensory Systems], *34*(2), 100-106. https://doi.org/10.31857/S0235009220020043

Joblove, G. H., & Greenberg, D. (1978). Color spaces for computer graphics. In: *SIGGRAPH '78. Proceedings of the 5th annual conference on Computer graphics and interactive techniques* (pp. 20-25). https://doi.org/10.1145/800248.807362

MacAdam, D. L. (Ed.). (1970). *Sources of color science*. MIT Press.

McKeefry, D. J., Murray, I. J., & Parry, N. R. (2007). Perceived shifts in saturation and hue of chromatic stimuli in the near peripheral retina. *Journal of the Optical Society of America A*, *24*(10), 3168-3179. https://doi.org/10.1364/JOSAA.24.003168

Mollon, J. D., Regan, B. C., & Bowmaker, J. K. (1998). What is the function of the cone-rich rim of the retina? *Eye*, *12*(3), 548-552. https://doi.org/10.1038/eye.1998.144

Moreland, J. D. (1972). Peripheral colour vision. In D. Jameson, & L. H. Hurvich (Eds.), *Handbook of sensory physiology, Vol. VII/4. Visual psychophysics* (pp. 517–536). Springer.

Moreland, J. D., & Cruz, A. (1959). Colour perception with the peripheral retina. *Optica Acta: International Journal of Optics*, *6*(2), 117-151. https://doi.org/10.1080/713826278

Murray, I. J., Parry, N. R. A., & McKeefry, D. J. (2006). Cone opponency in the near peripheral retina. *Visual Neuroscience*, *23*(3-4), 503. https://doi.org/10.1017/0S0952523806233315

Murray, I. J., Parry, N. R., McKeefry, D. J., & Panorgias, A. (2012). Sex-related differences in peripheral human color vision: a color matching study. *Journal of Vision*, *12*(1):18. https://doi.org/10.1167/12.1.18

Nagy, A. L., & Wolf, S. (1993). Red-green color discrimination in peripheral vision. *Vision research, 33*(2), 235-242. https://doi.org/10.1016/0042-6989(93)90161-O

Neitz, J., & Jacobs, G. H. (1990). Polymorphism in normal human color vision and its mechanism. *Vision Research*, *30*(4), 621-636. https://doi.org/10.1016/0042-6989(90)90073-T

Nerger, J. L., Volbrecht, V. J., & Ayde, C. J. (1995). Unique hue judgments as a function of test size in the fovea and at 20-deg temporal eccentricity. *Journal of the Optical Society of America A*, *12*(6), 1225-1232. https://doi.org/10.1364/JOSAA.12.001225

Noorlander, C., Koenderink, J. J., Den Olden, R. J., & Edens, B. W. (1983). Sensitivity to spatiotemporal colour contrast in the peripheral visual field. *Vision Research*, *23*(1): 1-11. https://doi.org/10.1016/0042-6989(83)90035-4

Opper, J. K., Douda, N. D., Volbrecht, V. J., & Nerger, J. L. (2014). Supersaturation in the peripheral retina. *Journal of the Optical Society of America A*, *31*(4), A148-A158. https://doi.org/10.1364/JOSAA.31.00A148

Østerberg, G. A. (1935). Topography of the layer of the rods and cones in the human retima. *Acta Ophthalmologica*, *13*(Supplement 6), 1-102.

Panorgias, A., Kulikowski, J. J., Parry, N. R., McKeefry, D. J., & Murray, I. J. (2012). Phases of daylight and the stability of color perception in the near peripheral human retina. *Journal of Vision*, 12(3), 1-1. https://doi.org/10.1167/12.3.1

Parry, N. R., McKeefry, D. J., & Murray, I. J. (2006). Variant and invariant color perception in the near peripheral retina. *Journal of the Optical Society of America A, 23*(7), 1586-1597. https://doi.org/10.1364/JOSAA.23.001586

Parry, N. R., Panorgias, A., McKeefry, D. J., & Murray, I. J. (2012). Real-world stimuli show perceived hue shifts in the peripheral visual field. *Journal of the Optical Society of America A*, *29*(2), A96-A101. https://doi.org/10.1364/JOSAA.29.000A96

Polyak, S. L. (1941). *The retina: The anatomy and the histology of the retina in man, ape, and monkey, including the consideration of visual functions, the history of physiological optics, and the histological laboratory technique*. University of Chicago Press.

Polymeropoulos, G., Bisketzis, N., & Topalis, F. (2011). A tetrachromatic model for colorimetric use in mesopic vision. *Color Research & Application*, *36*(2), 82-95. https://doi.org/10.1002/col.20603

Pyayt, A. (2020). Smartphones for rapid kits. In J.-Y. Yoon (Ed.), *Smartphone based medical diagnostics* (pp. 89-102). Academic Press. https://doi.org/10.1016/B978-0-12-817044-1.00006-5

Rozhkova, G. I., & Yarbus, A. L. (1974). Zavisimost' periferičeskogo zrenija ot skorosti smeščenija setčatočnogo izobraženija [The effects of velocity of retinal image movement on peripheral vision.] *Biofizika*, *19*(5), 908-912 (in Russian).

Rozhkova, G. I., Belokopytov, A. V., & Iomdina, E. N. (2019a). Present view of the human peripheral vision specifics. *Sensornye sistemy* [Sensory systems], *33*(4), 305-330. https://doi.org/10.1134/S0235009219040073 (in Russian)

Rozhkova, G. I., Iomdina, E. N., Selina, O. M., Belokopytov, A. V., & Nikolayev, P. P. (2019b). Contribution of the marginal peripheral retina to color constancy: evidence obtained due to contact lens with implanted occluder. *Sensornye sistemy* [Sensory Systems], *33*(2), 113-123. https://doi.org/10.1134/S0235009219020082 (in Russian)

Schein, S. J. (1988). Anatomy of macaque fovea and spatial densities of neurons in foveal representation. *Journal of Comparative Neurology, 269*, 479-505. https://doi.org/10.1002/cne.902690403

Schroeder, M. M., Harrison, K. R., Jaeckel, E. R., Berger, H. N., Zhao, X., Flannery, M. P., ..., & Wong, K. Y. (2018). The roles of rods, cones, and melanopsin in photoresponses of M4 intrinsically photosensitive retinal ganglion cells (ipRGCs) and optokinetic visual behavior. *Frontiers in Cellular Neuroscience*, *12*, 203. https://doi.org/10.3389/fncel.2018.00203

Smith, A. R. (1978). Color gamut transform pairs. *ACM SIGGRAPH Computer Graphics*, *12*(3), 12-19. https://doi.org/10.1145/965139.807361

Smith, V. C., & Pokorny, J. (2003). Color matching and color discrimination In S. K. Shevell (Ed.), *The science of color*, 2nd ed. (pp 103-142). Optical Society of America/Elsevier.

Solomon, S. G., & Lennie, P. (2007). The machinery of colour vision. *Nature Reviews Neuroscience*, *8*(4), 276-286. https://doi.org/10.1038/nrn2094

Spitschan, M. (2019). Melanopsin contributions to non-visual and visual function. *Current Opinion in Behavioral Sciences*, *30*, 67-72. https://doi.org/10.1016/j.cobeha.2019.06.004

Stabell, B., & Stabell, U. (1976). Rod and cone contributions to peripheral colour vision. *Vision Research, 16*(10), 1099-1104. https://doi.org/10.1016/0042-6989(76)90249-2

Stabell, B., & Stabell, U. (1979). Rod and cone contributions to change in hue with eccentricity. *Vision Research*, *19*(10), 1121-1125. https://doi.org/10.1016/0042-6989(79)90007-5

Stabell, U., & Stabell, B. (1982a). Color vision in the peripheral retina under photopic conditions. *Vision Research*, *22*(7), 839-844. https://doi.org/10.1016/0042-6989(82)90017-7

Stabell, B., & Stabell, U. (1982b). Bezold-Brücke phenomenon of the far peripheral retina. *Vision Research*, *22*(7), 845-849. https://doi.org/10.1016/0042-6989(82)90018-9

Stabell, U., & Stabell, B. (1984). Color-vision mechanisms of the extrafoveal retina. *Vision Research*, *24*(12), 1969-1975. https://doi.org/10.1016/0042-6989(84)90032-4

Stabell, B., & Stabell, U. (1996). Peripheral colour vision: effects of rod intrusion at different eccentricities. *Vision Research*, *36*(21), 3407-3414. https://doi.org/10.1016/0042-6989(96)00079-X

Stabell, B., & Stabell, U. (2002). Effects of rod activity on color perception with light adaptation. *Journal of the Optical Society of America A, 19*(7), 1249-1258. https://doi.org/10.1364/JOSAA.19.001249

To, M. P. S., Regan, B. C., Wood, D., & Mollon, J. D. (2011). Vision out of the corner of the eye. *Vision Research*, *51*(1), 203-214. https://doi.org/10.1016/j.visres.2010.11.008

Toscani, M., Gil, R., Guarnera, D., Guarnera, G. C., Kalouaz, A., & Gegenfurtner, K. R. (*2019*). Assessment of OLED head mounted display for vision research with virtual reality. *15th International*

Conference on Signal-Image Technology & Internet-Based Systems (SITIS), pp. 738-745, https://doi.org/10.1109/SITIS.2019.00120.

Trezona, P. W. (1970). Rod participation in the 'blue' mechanism and its effect on colour matching. *Vision Research*, *10*(4), 317-332. https://doi.org/10.1016/0042-6989(70)90103-3

Trezona, P. W. (1973). The tetrachromatic colour match as a colorimetric technique. *Vision Research*, *13*(1), 9-25. https://doi.org/10.1016/0042-6989(73)90161-2

Trezona, P. W. (1974). Additivity in the tetrachromatic colour matching system. *Vision Research*, *14*(12), 1291-1303. https://doi.org/10.1016/0042-6989(74)90001-7

Troxler, D. I. P. V. (1804). Ueber das Verschwinden gegebener Gegenstande innerhalb unseres Gesichtskreises. *Ophthalmologische Bibliothek*, *2*, 1-119. (in German)

Tyler, C. W. (2015). Peripheral color demo. *i-Perception*, *6*(6). https://doi.org/10.1177/2041669515613671

Tyler, C. W. (2016). Peripheral color vision and motion processing. *Electronic Imaging*, *2016*(16), 1-5. https://doi.org/10.2352/ISSN.2470-1173.2016.16.HVEI-138

van Esch, J. A., Koldenhof, E. E., Van Doorn, A. J., & Koenderink, J. J. (1984). Spectral sensitivity and wavelength discrimination of the human peripheral visual field. *Journal of the Optical Society of America A*, *1*(5), 443-450. https://doi.org/10.1364/JOSAA.1.000443

Volbrecht, V. J., & Nerger, J. L. (2012). Color appearance at $\pm 10^{\circ}$ along the vertical and horizontal meridians. *Journal of the Optical Society of America A*, *29*(2), A44. https://doi.org/10.1364/josaa.29.000a44

Williams, R. W. (1991). The human retina has a cone-enriched rim. *Visual Neuroscience*, *6*(4), 403-406. https://doi.org/10.1017/S0952523800006647.

World Medical Association Declaration of Helsinki: Ethical Principles for Medical Research Involving Human Subjects. (2013). JAMA, 310(20):2191–2194. https://doi.org/10.1001/jama.2013.281053

Wright, W. D. (1929). A re-determination of the trichromatic coefficients of the spectral colours. *Transactions of the Optical Society*, *30*(4), 141-164. https://doi.org/10.1088/1475-4878/30/4/301

Wyszecki, G., & Stiles, W. (1982). *Color science: concepts and methods, quantitative data and formulae*, 2nd ed. Wiley.

Yamakawa, M., Tsujimura, S. I., & Okajima, K. (2019). A quantitative analysis of the contribution of melanopsin to brightness perception. *Scientific Reports*, *9*(1):7568. https://doi.org/10.1038/s41598-019-44035-3

Yarbus, A. L., & Rozhkova, G. I. (1977). The peculiarities of perceiving visual objects at the periphery of the visual field. *Sensornye sistemy* [Sensory systems], 64-73. (in Russian).

Zele, A. J., Feigl, B., Adhikari, P., Maynard, M. L., & Cao, D. (2018). Melanopsin photoreception contributes to human visual detection, temporal and colour processing. *Scientific Reports*, *8*(1):3842. https://doi.org/10.1038/s41598-018-22197-w

Open Practices Statement The code and data of the study are available to the research community use at https://github.com/abelokopytov/spot. None of the experiments was preregistered.